

FakeReasoning: Towards Generalizable Forgery Detection and Reasoning

Yueying Gao¹ Dongliang Chang^{2†} Bingyao Yu²
Haotian Qin¹ Lei Chen² Kongming Liang¹ Zhanyu Ma¹

¹PRIS, Beijing University of Posts and Telecommunications

²Tsinghua University

Abstract

Accurate and interpretable detection of AI-generated images is essential for mitigating risks associated with AI misuse. However, the substantial domain gap among generative models makes it challenging to develop a generalizable forgery detection model. Moreover, since every pixel in an AI-generated image is synthesized, traditional saliency-based forgery explanation methods are not well suited for this task. To address these challenges, we propose modeling AI-generated image detection and explanation as a Forgery Detection and Reasoning task (FDR-Task), leveraging vision-language models (VLMs) to provide accurate detection through structured and reliable reasoning over forgery attributes. To facilitate this task, we introduce the Multi-Modal Forgery Reasoning dataset (MMFR-Dataset), a large-scale dataset containing 100K images across 10 generative models, with 10 types of forgery reasoning annotations, enabling comprehensive evaluation of FDR-Task. Additionally, we propose FakeReasoning, a forgery detection and reasoning framework with two key components. First, Forgery-Aligned Contrastive Learning enhances VLMs' understanding of forgery-related semantics through both cross-modal and intra-modal contrastive learning between images and forgery attribute reasoning. Second, a Classification Probability Mapper bridges the optimization gap between forgery detection and language modeling by mapping the output logits of VLMs to calibrated binary classification probabilities. Experiments across multiple generative models demonstrate that FakeReasoning not only achieves robust generalization but also outperforms state-of-the-art methods on both detection and reasoning tasks.

1. Introduction

The rapid advancement of deep generative models has enabled AI to produce highly realistic images [10, 27, 38, 40],

raising concerns about AI misuse, particularly in misinformation dissemination. Recent studies have shown that AI-generated content has been widely used in political propaganda, financial fraud, and social media manipulation, underscoring the urgent need for reliable detection mechanisms [19, 45]. Accurate and interpretable detection of AI-generated images is essential for mitigating these risks. However, existing detection methods face two key challenges. First, AI-generated images from different models exhibit distinctive artifacts, leading to a substantial domain gap that limits the generalization ability of detectors trained on specific generative models. Second, unlike traditional image manipulation methods [26, 34, 50, 51, 57] that modify only specific regions, every pixel in an AI-generated image is synthesized, rendering saliency-based explainability methods [11, 14, 15, 42] ineffective. These challenges highlight the need for a generalizable and interpretable AI-generated image detector capable of understanding forgery attributes beyond model-specific patterns.

Prior research has attempted to address these issues using two primary strategies: 1) low-level feature analysis focuses on detecting common fingerprints present across generative models [3, 5, 53, 55, 61], but these methods suffer from severe domain shift, as training on one set of generative models does not generalize well to unseen model sets; 2) high-level semantics has recently been explored using vision-language models (VLMs) to detect semantics inconsistencies within AI-generated images [4, 32, 35, 60]. However, due to the task gap between VLMs' pretraining objectives and AI-generated image detection, they lack sensitivity to forgery artifacts, leading to suboptimal detection performance. Furthermore, while multi-modal large language models (MLLMs) have demonstrated some ability to explain partially manipulated images [25, 59, 64], they fail to provide structured reasoning for fully AI-generated images, limiting their real-world applicability.

To overcome these limitations, in this paper, we propose modeling AI-generated image detection and explanation as a Forgery Detection and Reasoning task (FDR-Task), leveraging vision-language models (VLMs) to per-

† Corresponding author

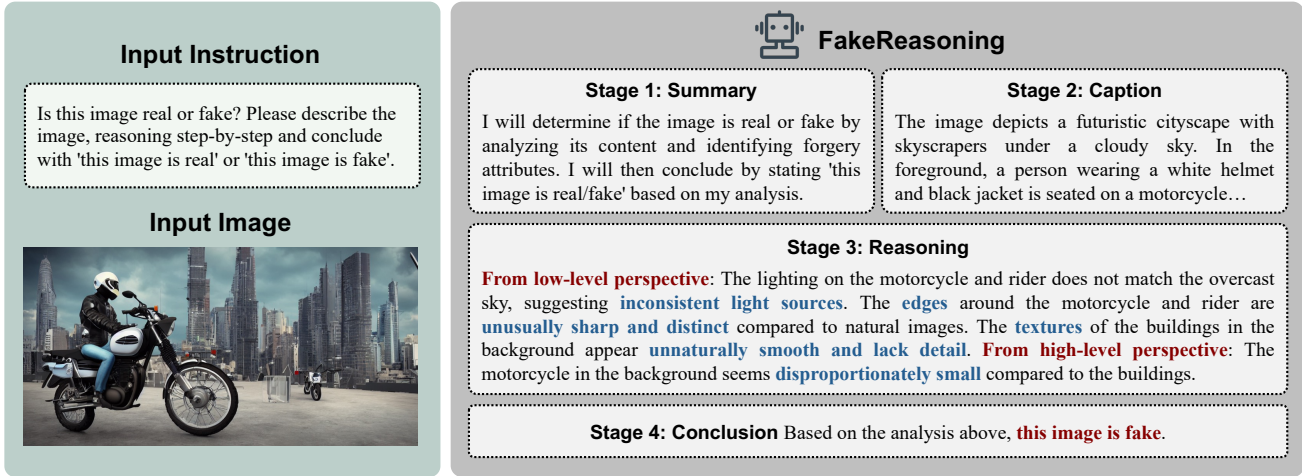


Figure 1. Illustration of the forgery detection and reasoning task. Different from existing forgery detection, the FDR-Task simultaneously assesses image authenticity and analyze forgery-related attributes, improving both detection accuracy and interpretability.

form accurate detection through structured and reliable reasoning over forgery attributes. As shown in Figure 1, FDR-Task enables VLMs to simultaneously assess image authenticity and analyze forgery-related attributes, improving both detection accuracy and interpretability. To facilitate this task, we introduce the Multi-Modal Forgery Reasoning Dataset (MMFR-Dataset), a large-scale dataset containing 100K images across 10 generative models, with 10 types of forgery reasoning annotations. Unlike existing datasets that focus solely on a single visual modality, MMFR-Dataset provides structured reasoning annotations, allowing VLMs to systematically interpret forgery attributes. We construct MMFR-Dataset using a Forgery Interpretation Prompt, instructing GPT-4o to extract fine-grained forgery attributes. We further introduce a structured chain-of-thought reasoning framework, compiling GPT-4o-assisted interpretations into hierarchical reasoning steps. With structured reasoning annotations and labeled images, MMFR-Dataset bridges the gap between detection and interpretability and enables a comprehensive evaluation of the FDR-Task.

Building upon MMFR-Dataset, we propose FakeReasoning, a forgery detection and reasoning framework that enhances both detection accuracy and interpretability. FakeReasoning introduces two key components. First, Forgery-Aligned Contrastive Learning (FACL) strengthens VLMs’ understanding of forgery-related semantics through both cross-modal and intra-modal contrastive learning between images and forgery attribute reasoning, enhancing the reasoning capability of vision-language models. Second, a Classification Probability Mapper (CPM) bridges the optimization gap between forgery detection and language modeling by mapping the output logits of VLMs to calibrated binary classification probabilities, improving detection accuracy and VLMs’ sensitivity to subtle forgeries. Unlike

conventional approaches that rely on model-specific low-level fingerprints, FakeReasoning establishes a classification boundary between real and AI-generated images based on forgery attributes, enhancing generalization across unseen generative models and mitigating domain asymmetry.

2. Related Work

Generalizable Forgery Detection. With the advent of diverse deep generative models, designing detectors that generalize to unseen generative domains is essential. CNNDetection [53] shows that detectors trained on ProGAN [21] images generalize well across various GANs. DIRE [55] reveals that diffusion-model-generated images can be effectively reconstructed using diffusion models, while real images are not. Although these methods achieve good intra-domain generalization, they struggle with unseen domains. Recently, high-level semantics have been explored using vision-language models (VLMs) to detect AI-generated images. UniDF [35] employs a frozen CLIP visual encoder to avoid mode asymmetry. FatFormer [32] utilizes zero-shot inference from CLIP [37], enhancing prompt templates. However, due to the task gap between VLMs’ pretraining objectives and forgery detection, VLMs lack sensitivity to subtle forgeries, leading to suboptimal performance. Additionally, AntifakePrompt [4] redefines forgery detection as a visual question answering task, using prompt tuning to fine-tune InstructBLIP [9]. Bi-LORA [22] approaches forgery detection as an image captioning task, using LoRA [18] to fine-tune BLIP-2 [24]. These methods overlook the gap between language modeling and forgery detection, failing to fully exploit the interpretive capabilities of VLMs in forgery detection.

Vision-Language Models. To effectively leverage unimodal large models and bridge the gap between modal-

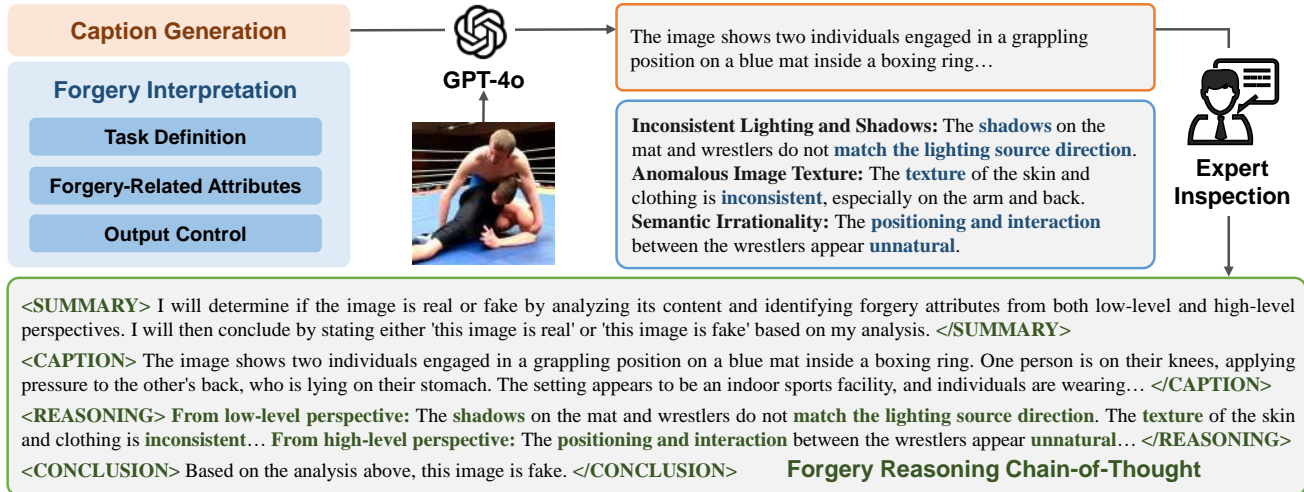


Figure 2. Illustration of the construction flow of MMFR-Dataset. GPT-4o is tasked with caption generation and forgery interpretation. For the forgery interpretation task, a tailored prompt is crafted to guide GPT-4o in describing forgery-related attributes. After inspected by human experts, the generated captions and interpretations are compiled with a chain-of-thought approach to enhance structured reasoning.

ities, various vision-language models have been developed. BLIP-2 [24] introduces a lightweight transformer, Q-Former, which learns text-relevant image features from a frozen visual encoder. LLaVA [31] employs a linear layer to map visual embeddings into the text embedding space. However, due to the domain gap between the pretraining data of VLMs and AI-generated media, these models struggle to understand forgery-related concepts such as “real”, “fake” or “AI-generated” [28], which are crucial for forgery reasoning tasks.

3. Multi-Modal Forgery Reasoning Dataset

Most existing forgery detection datasets focus on a single visual modality [53, 67, 68]. Some multi-modal datasets include text-guided images and descriptive captions [43, 56], but these are inadequate for forgery reasoning tasks. Therefore, we introduce the MMFR-Dataset, a large-scale synthetic image dataset with detailed reasoning on forgery-related attributes. MMFR-Dataset features a comprehensive training set and diverse evaluation sets. All reasoning results are generated by well-instructed GPT-4o and structured through step-by-step reasoning chains, enabling both detection and reasoning tasks.

3.1. Source Image collection

Training set: For generalizable forgery detection, we follow the training paradigm of [31, 35, 53] and collect training set on one kind of generative model. To guarantee the diversity and quality of training data, we choose DiffusionDB dataset [56] for fake images and LAION-Aesthetics [41] for real images.

Evaluation sets: In order to comprehensively evaluate the

generalization of forgery detectors, we collect and organize the open-source AI-generated image datasets. Evaluation sets consist of up-to-date generative models of five diffusion models and five Generative Adversarial Networks. The real and fake images from each generative model are equal in number and follow similar distributions. Detailed information of evaluation sets are summarized in Table 1.

3.2. Forgery Reasoning Generation

Forgery reasoning in MMFR-Dataset is generated in two steps. First, we design a *Forgery Interpretation Prompt* and employ GPT-4o to interpret specific attributes signifying the image authenticity. Second, we decompose forgery reasoning process into four structured stages and compile corresponding answers of each stage into MMFR-Dataset. The construction flow is shown in Figure 2.

GPT-4o Assisted Forgery Interpretation. GPT-4o has proven its capabilities in detecting and interpreting potential forgeries within images [28, 65]. Compared to manual analysis, using GPT-4o for automated annotation significantly reduces time costs while expanding the size of datasets [31, 59]. To generate correct and comprehensive interpretations of forgery-related attributes, we design a *Forgery Interpretation Prompt* considering following aspects :

- **Task Definition:** First of all, *Prompt* specifies the image authenticity as either “real” or “fake”. GPT-4o is tasked with identifying specific attributes that signify the image authenticity and providing detailed descriptions.
- **Forgery-Related Attributes Prior:** *Prompt* includes a comprehensive set of attributes widely used in image forensics, ranging from low-level artifacts to high-level semantics, to guide GPT-4o’s interpretation.
- **Output Control:** *Prompt* defines a standard output format

Generative Models	Year	Size	Real Images	Sources
GLIDE	2021	2K	LAION	both from [35]
Guided	2022	2K	ImageNet	both from [35]
Stable Diffusion	2022	2K	LAION	fake from [56] real from [35]
DALLE-3	2023	2K	LAION	fake from [17] real from [41]
DeepFloyd IF	2023	2K	LAION	fake from [4] real from [41]
BigGAN	2018	2K	ImageNet	fake from [53] real from [53]
GauGAN	2019	2K	COCO	both from [53]
StyleGAN2	2019	2K	Celeba-HQ	both from [48]
StyleGAN-XL	2022	2K	ImageNet	fake from [4] real from [39]
GigaGAN	2023	2K	ImageNet	both from [8]

Table 1. Evaluation sets. The evaluation sets contain comprehensive, balanced, and high-quality synthetic images for evaluating generalization of forgery detectors.

including authenticity labels and attribute interpretations. Besides, it also specifies a distinct output for failure cases where GPT-4o is unable to ascertain the image authenticity. Such outputs are filtered out after generation.

Please refer to Appendix for full-text *Forgery Interpretation Prompt*. Upon generation, interpretations on forgery-related attributes are reviewed by experts. And invalid annotations are filtered out.

Forgery Reasoning Chain-of-Thought. Inspired by recent research in multi-modal chain-of-thought [6, 44, 58], we develop a specific chain-of-thought for forgery reasoning task, consisting of structured stages and hierarchical steps, to enhance visual reasoning capability of VLMs. First, we decompose forgery reasoning process into four stages:

- **Summary:** In this stage, *Forgery Reasoning CoT* provides a brief summary of the proposed task and explains the steps of reasoning process.
- **Caption:** *Forgery Reasoning CoT* gives a description of elements and relations within an image to help understand image and find forgeries.
- **Reasoning:** From both low-level and high-level perspectives, *Forgery Reasoning CoT* identify forgery-related attributes and decide the authenticity of the input image.
- **Conclusion:** Based on above stages, *Forgery Reasoning CoT* outputs the final decision on image authenticity.

To emphasize structured reasoning stages, we use four pairs of special `<SEG>` tags: `<SUMMARY></SUMMARY>`, `<CAPTION></CAPTION>`, `<REASONING></REASONING>` and `<CONCLUSION></CONCLUSION>` at both beginning and end of each stage. Summary and conclusion are pre-defined for forgery reasoning task. Caption is generated by GPT-4o and reasoning is compiled from GPT-4o as-

sisted forgery interpretation. Upon training on MMFR-Dataset, vision-language models are able to conduct structured forgery reasoning in four stages without external prompt engineering.

3.3. Dataset Statistics

The training set consists of 50,268 synthetic images with 129,351 reasoning annotations, and 50,909 real images with 183,245 reasoning annotations. Across all annotations, there are 10 types of forgery-related attributes, whose distributions in real and fake images are depicted in Appendix. The evaluation sets comprise 10,000 synthetic images with 25,356 reasoning annotations and 10,000 real images with 37,050 reasoning annotations, providing a robust foundation for a comprehensive evaluation of both the forgery detection and reasoning tasks.

4. Method

4.1. Overall Framework

Inspired by the revolutionary advancements in vision-language models [2, 7, 30], we aim to leverage their image understanding and text generation capabilities to analyze image authenticity and provide reliable explanations. In Section 3, we introduce the MMFR-Dataset for fine-tuning VLMs but there still exists several challenges. Firstly, due to the domain gap between VLMs’ pretraining data and AI-generated media, these models struggle with understanding forgery-related concepts, which are crucial for forgery reasoning task. Secondly, the task gap between VLMs’ pretraining objectives and forgery detection results in a lack of sensitivity to forgery artifacts, leading to suboptimal detection performance. To address these gaps and tailor VLMs for the FDR-Task, we propose FakeReasoning, which includes two key components: FACL and CPM, as illustrated in Figure 3.

Specifically, we use images and forgery reasoning from the MMFR-Dataset as the visual input X_v and answers X_a . The question X_q , such as the Forgery Detection and Reasoning Prompt, is defined in Figure 3. Image embeddings F_v are extracted using the CLIP visual encoder and a projection layer W , while the question and answer are encoded into language embeddings F_q and F_a . The question embeddings F_q and image embeddings F_v are initially input into the large language model, which is optimized with F_a and language modeling. To enhance VLMs’ understanding of forgery-related semantics, FACL aligns image embeddings F_v and forgery reasoning embeddings F_a through cross-modal and intra-modal contrastive learning, thereby enhancing the reasoning capability of vision-language models. Furthermore, to bridge the optimization gap between forgery detection and language modeling, CMP first locates the *classification index* of output logits through pattern

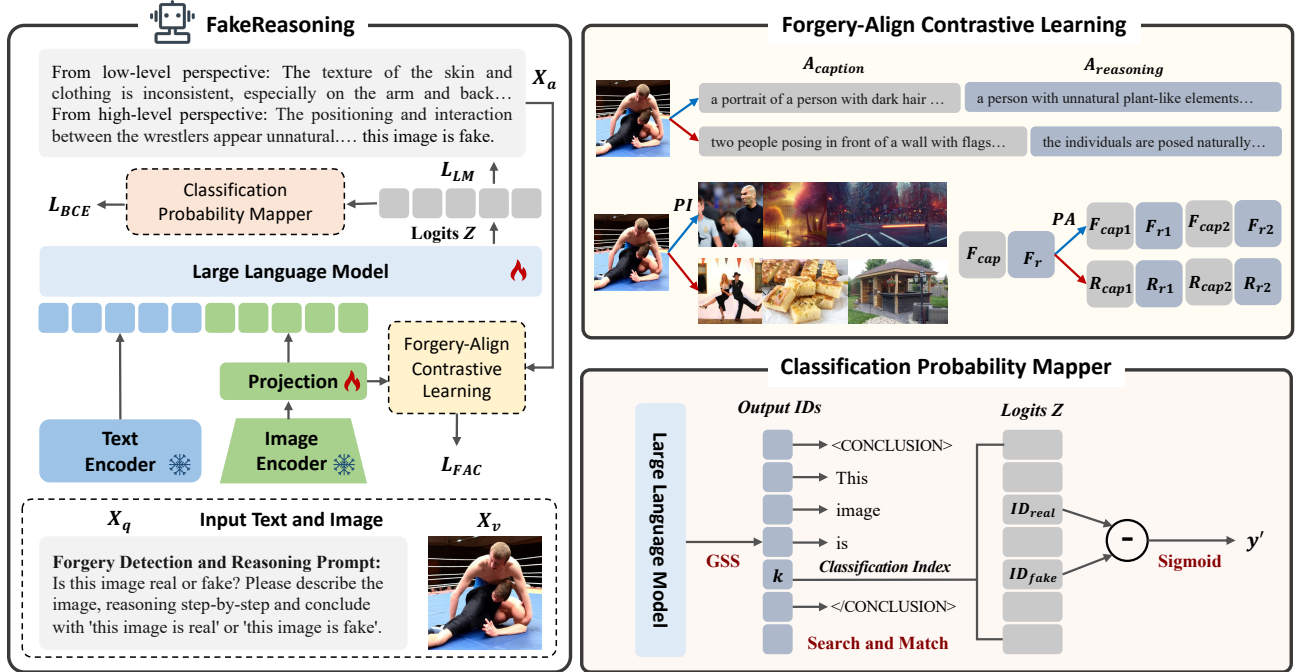


Figure 3. The pipeline of the proposed FakeReasoning. FakeReasoning performs language modeling task to fine-tune the vision-language model on the MMFR-dataset. Meanwhile, Forgery-Align Contrastive Learning is performed on both cross-modal and intra-modal to enhance VLM’s understanding of forgery-related semantic. Classification Probability Mapper is designed to map the logits outputs to binary classification probability, bridging the optimization gap between forgery detection and language modeling.

matching and maps the corresponding logits to binary classification probabilities, ensuring more reliable detection.

4.2. Forgery-Align Contrastive Learning

Vision-language models are pretrained on web-scale image-text pairs and demonstrate outstanding performance on downstream tasks that rely on high-level semantics, such as visual question answering [52, 62, 66] and image-text retrieval [33, 54, 63]. However, these models struggle to comprehend forgery-related concepts due to non-specific training data [20]. Therefore, we implement both cross-modal and intra-model forgery-align contrastive learning between images and forgery attribute reasoning to enhance the models’ understanding of forgery-related semantics.

Cross-Modal Contrastive Learning. To simplify the formulations, we use (I, Q, A) represents the model input (X_v, X_q, X_a) , where A is divided into four stages $(A_s, A_{cap}, A_r, A_{con})$. To further align image forgeries and related semantics, we employ cross-modal contrastive learning on the triplet (I, A_{cap}, A_{con}) , which pulls the matched caption and reasoning towards the image and pushes unmatched ones apart, emphasizing both content semantics and forgery-related semantics simultaneously. The positive and negative samples are illustrated in Figure 3.

Following the InfoNCE loss [36], the cross-modal con-

trastive learning from image to answer is defined as:

$$\mathcal{L}_{v2a}(I, A) = -\log \frac{\exp(S(I, A^+)/\tau)}{\sum_{A_i \in A} \exp(S(I, A_i)/\tau)}, \quad (1)$$

where $A = (A^+, A^-)$. Here, A^+ represents the matched caption and reasoning corresponding to the image I , while A^- denotes the unmatched ones. We apply average pooling to obtain global features for the similarity matrix calculation, $S(I, A) = \text{AvgPool}(F_v)^T \cdot \text{AvgPool}(F_a)$. To incorporate more positive and negative samples for contrastive learning, we follow [16] and utilize two queues to store the most recent n embeddings of images, captions, and reasoning. The parameter τ is a trainable temperature hyperparameter, initially set to 0.07. Similarly, the cross-modal contrastive learning from answer to image is formulated as:

$$\mathcal{L}_{a2v}(A, I) = -\log \frac{\exp(S(A, I^+)/\tau)}{\sum_{I_i \in I} \exp(S(A, I_i)/\tau)}, \quad (2)$$

where $I = (I^+, I^-)$. I^+ represents the matched images, while I^- denotes the unmatched ones.

Intra-Modal Contrastive Learning. In proposed FDR-Task, uni-modal data contains class labels to develop task-specific positive and negative examples, referred to as hard examples in contrastive learning, which are crucial for effective training. Inspired by [23], we perform image-modal

supervised contrastive learning as follows:

$$\mathcal{L}_{v2v}(I) = -\frac{1}{|PI|} \sum_{I_i^+ \in PI} \log \frac{\exp(S(I, I_i^+)/\tau)}{\sum_{I_i \in I} \exp(S(I, I_i)/\tau)}, \quad (3)$$

where the set PI represents the positive samples for the anchor image I and is constructed from the image queue based on the authenticity of I . Through supervised contrastive learning, images belonging to the same class are pulled closer in the embedding space, while images from different classes are pushed apart. Similarly, text-modal supervised contrastive learning is conducted as follows:

$$\mathcal{L}_{a2a}(A) = -\frac{1}{|PA|} \sum_{A_i^+ \in PA} \log \frac{\exp(S(A, A_i^+)/\tau)}{\sum_{A_i \in A} \exp(S(A, A_i)/\tau)}, \quad (4)$$

where the set PA comprises positive samples for the anchor A and is constructed based on the text queue and the anchor authenticity. Forgery-Aligned Contrastive Loss is the average of above four losses:

$$\mathcal{L}_{FAC} = \frac{1}{4}[\mathcal{L}_{v2a}(I, A) + \mathcal{L}_{a2v}(A, I) + \mathcal{L}_{v2v}(I) + \mathcal{L}_{a2a}(A)]. \quad (5)$$

4.3. Classification Probability Mapper

The training objective of vision-language models is to minimize the discrepancy between predicted texts and input texts, a process known as language modeling. Although the predicted texts can indicate the image authenticity, there exists an optimization gap between forgery detection and language modeling, leading to suboptimal detection performance in fine-tuned VLMs [4, 22]. Moreover, in addition to high-level semantics, FDR-Task also emphasizes low-level features to detect subtle forgeries. To address these challenges, we propose the Classification Probability Mapper (CPM), which first locates the *classification index* of output logits through pattern matching and maps the corresponding logits to binary classification probabilities, improving detection accuracy and VLMs’ sensitivity to subtle forgeries.

Given the input image embedding F_v and question embedding F_q , the final layer of the vision-language model outputs the logits $Z = (Z_1, Z_2, \dots, Z_N)$, representing the predicted probabilities for each token in the vocabulary. Here, $Z_i = (Z_{i1}, Z_{i2}, \dots, Z_{iV})$, where N is the length of the output sequence and V is the size of the vocabulary. Using the Greedy Search Strategy [47], we sample the predicted words based on the highest probabilities and obtain the output IDs $O = (O_1, O_2, \dots, O_N)$:

$$O_i = \arg \max_j (Z_{ij}). \quad (6)$$

According to the *Forgery Reasoning CoT*, image authenticity is determined in the conclusion stage. Therefore, we encode `<CONCLUSION>` and answer template “This image is” into token IDs as the match pattern p . We use this pattern

to search through the output IDs and identify the subsequent index k :

$$k = \{m + l \mid O_{m:m+l} = p, m \in [0, N - l]\}, \quad (7)$$

where l is the length of pattern p . k is referred to as *classification index*. The token probability at this index indicates whether the input image is “real” or “fake”.

As a binary classification task, the probabilities of an image being classified as “real” or “fake” must sum to 1. Consequently, we index the token probabilities for both the “real” and “fake” IDs, utilizing their difference as the classification probability for forgery detection. The final prediction is computed as follows:

$$y' = \text{sigmoid}[(Z_{k, ID_{fake}} - Z_{k, ID_{real}})/\tau], \quad (8)$$

where τ is a trainable temperature hyperparameter to smooth the probability distribution, initially set to 10. Following [13, 35, 53], binary cross-entropy loss is employed for forgery detection task:

$$\mathcal{L}_{BCE} = -(y \cdot \log(y') + (1 - y) \cdot \log(1 - y')), \quad (9)$$

where y is the ground truth of image authenticity.

4.4. Joint Optimization

Following the methodology of LLaVA [31], the language modeling task is optimized using an auto-regressive training objective:

$$\mathcal{L}_{LM} = -\sum_{i=1}^L \log p_{\theta}(x_i | X_v, X_{q, <i}, X_{a, <i}), \quad (10)$$

where θ represents the trainable parameters of the large language model. $X_{q, <i}$ and $X_{a, <i}$ denote the question and answer tokens from all previous turns prior to the current prediction token x_i , and L is the sequence length. During training, FakeReasoning is optimized through joint losses:

$$\text{Loss} = \mathcal{L}_{FAC} + \mathcal{L}_{BCE} + \mathcal{L}_{LM}. \quad (11)$$

The visual encoder remains frozen while we update the parameters in the projection layer and the large language model. Please refer to the Appendix for an ablation study on fine-tuning modules.

5. Experiment

5.1. Settings

State-of-the-Art Methods. To evaluate detection performance, we compare our approach with several CLIP-based methods, including CNNDetection [53], UniFD [35], DEFAKE [43], AIDE [60], the VLM-based method Antifake-Prompt [4] and diffusion-reconstruction-based DIRE [55].

Method	Diffusion Models					Generative Adversarial Networks					AVG
	GLIDE	Guided	SD	DALLE-3	IF	BigGAN	GauGAN	SG2	SG-XL	GigaGAN	
CNNDetection [53]	51.75	43.60	85.55	79.45	73.10	47.90	44.60	47.70	59.20	49.05	58.19
DIRE [55]	55.00	50.90	99.80	60.20	<u>94.70</u>	50.20	50.60	47.80	56.90	74.10	64.02
UniDF [35]	81.55	63.80	94.75	<u>91.30</u>	84.60	69.45	82.20	55.65	73.60	68.70	76.56
DE-FAKE [43]	57.45	52.33	50.10	61.40	66.45	43.30	42.55	46.90	66.05	67.60	55.41
AntifakePrompt [4]	<u>94.70</u>	70.05	95.20	91.05	87.20	69.30	<u>84.25</u>	<u>61.10</u>	69.45	63.70	78.60
AIDE [60]	93.50	<u>74.15</u>	98.15	90.00	75.00	<u>86.75</u>	83.30	<u>58.95</u>	<u>82.35</u>	<u>75.25</u>	81.74
FakeReasoning	97.70	87.20	<u>99.20</u>	92.30	97.50	89.30	88.90	81.80	89.10	86.80	90.98

Table 2. Comparison on forgery detection. We retrain all state-of-the-art methods on the MMFR training set and test them on the MMFR evaluation sets. Image-level accuracy is reported for each evaluation set. SD, IF, SG2, SG-XL represent Stable Diffusion, DeepFloyd IF, StyleGAN2 and StyleGAN-XL. FakeReasoning outperforms all state-of-the-art methods, achieving an average accuracy of 90.98%

All state-of-the-art detectors are retrained on the MMFR-Dataset to ensure a fair comparison. Furthermore, to assess reasoning performance, we utilize open-source vision-language models such as LLaVA-1.5 [29], Qwen-2.5-VL [2], InstructBLIP [9], and InternVL-2.5 [7], alongside the commercial models GPT-4o [1] and GeminiPro [49].

Evaluation Metrics. For the forgery detection task, we report image-level accuracy (ACC), which is calculated based on the authenticity decisions in the conclusion stage. For the forgery reasoning task, we utilize the output from the reasoning stage for comparison. The generated reasoning results are assessed for similarity to the ground truth using BLEU-1/2 [28], ROUGE-L [28] and Semantic Similarity (CSS) [60].

Method	Detection			Reasoning			
	DM	GAN	AVG \uparrow	B-1 \uparrow	B-2 \uparrow	R-L \uparrow	CSS \uparrow
LLaVA-1.5 [29]	71.94	72.34	72.14	0.23	0.10	0.20	0.54
Qwen-2.5-VL [2]	65.75	57.72	61.74	0.22	0.09	0.19	0.56
InstructBLIP [9]	56.86	61.71	59.28	0.08	0.02	0.12	0.49
InternVL-2.5 [7]	71.42	60.94	66.18	0.14	0.08	0.16	0.58
GPT-4o [1]	<u>88.06</u>	<u>84.80</u>	<u>86.43</u>	<u>0.28</u>	<u>0.14</u>	<u>0.22</u>	<u>0.63</u>
GeminiPro [49]	66.00	71.60	68.80	0.17	0.09	0.18	0.51
FakeReasoning	94.78	87.18	90.98	0.36	0.24	0.34	0.77

Table 3. Comparison on the FDR-Task. We employ GPT-4o-assisted forgery interpretation as the ground truth and assess the quality of forgery reasoning. FakeReasoning consistently achieves superior performance in both detection and reasoning tasks.

Implementation Details. We select LLaVA-1.5-13b as the base VLM. The large language model is fine-tuned using LoRA [18] with a rank of 128 and a scaling factor of 256, while the projection layer is fully parameterized. We utilize the Adam optimizer with a learning rate of 2×10^{-4} and a cosine learning rate schedule with a 3% warmup ratio. The batch size is set to 4, and the model is trained on 4 RTX 4090 GPUs for only 1 epoch. During inference, the temperature is set to 0.2 for reasoning generation.

5.2. Benchmark for FDR-Task

Comparison on Forgery Detection. We first conduct a comprehensive comparison on the generalization of detection task. Specifically, we retrain all state-of-the-art methods with their official code on the MMFR training set and test them on the MMFR evaluation sets. For all experiments, we utilize the Forgery Detection and Reasoning Prompt, as illustrated in Figure 3, to query vision-language models. The results, presented in Table 2, include image-level accuracy for each evaluation set. Our method outperforms all state-of-the-art methods, with an average accuracy exceeding the suboptimal method AIDE [60] by 9.24%. DIRE [55] performs well on both Stable Diffusion and DeepFloyd IF. However, it falls to random guessing on other evaluation sets due to domain gaps and unexpected overfitting of JPEG artifacts [3]. In terms of generalization, AIDE [60] and AntifakePrompt [4] perform well on diffusion-model-generated images but experience significant drops on GAN-generated images. In contrast, FakeReasoning achieves the highest accuracy in 9 out of 10 generative models and shows the smallest variation in accuracy across different models. With powerful prior knowledge of vision-language model and task-specific fine-tuning, our model learns the correlation between forgery semantics and image features, instead of specific fingerprints [35], which contributes to strong detection generalization on unseen domains.

Comparison on Forgery Detection and Reasoning. To establish a foundational study for the FDR-Task, we employ GPT-4o-assisted forgery interpretation as the ground truth and assess the quality of forgery reasoning. The results are presented in Table 3. FakeReasoning consistently achieves superior performance in both detection and reasoning tasks. Representing commercial vision-language models, GPT-4o demonstrates remarkable zero-shot capabilities. Additionally, LLaVA-1.5 stands out among open-source vision-language models and is selected as the base VLM for the proposed FakeReasoning. In contrast, InstructBLIP exhibits noticeably low performance on reason-

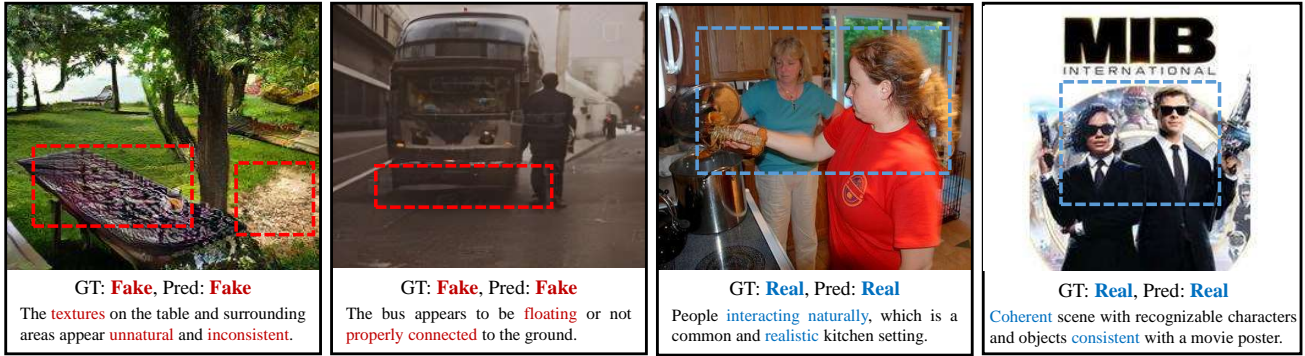


Figure 4. Visualization of FakeReasoning. The regions identified by forgery reasoning are highlighted with dashed boxes.

Variants	DM	GAN	AVG \uparrow	CSS \uparrow
LLaVA-1.5	71.94	72.34	72.14	0.54
Ours w/o Reasoning	89.33	78.00	85.56	0.42
Ours w/o Reasoning CoT	92.33	79.67	88.11	0.64
Ours w/ Reasoning CoT	94.78	88.90	91.84	0.77

Table 4. Ablation study of forgery reasoning task.

ing tasks. When using the original Forgery Detection and Reasoning Prompt, InstructBLIP tends to provide simplistic outputs like “This image is real/fake” without any detailed reasoning.

5.3. Ablation Study

Ablation Study of Forgery Reasoning Task. We designed the following variants: (1) LLaVA-1.5: zero-shot inference of LLaVA. (2) Ours w/o Reasoning: “This image is real/fake.” as the output ground truth. (3) Ours w/o Reasoning CoT: GPT-4o-assisted forgery interpretation as the output ground truth. (4) Ours w/ Reasoning CoT: the proposed FakeReasoning, using a forgery reasoning CoT as the output ground truth. The performance of these variants is shown in Table 4. Both reasoning and structured reasoning enhance the forgery detection task, particularly for GAN-generated images. The reasoning task helps vision-language models establish classification boundary through forgery semantics rather than specific artifacts, thereby enhancing generalization across unseen generative models. Moreover, the structured chain-of-thought approach effectively improves the quality of forgery reasoning.

Ablation Study of Losses. To illustrate the role of each proposed loss, we incrementally add \mathcal{L}_{FAC} and \mathcal{L}_{BCE} to \mathcal{L}_{LM} . The corresponding results for each case are shown in Table 5. When \mathcal{L}_{FAC} is added to the baseline, the quality of the reasoning task significantly improves, demonstrating the effectiveness of Forgery-Align Contrastive Learning. Incorporating \mathcal{L}_{BCE} results in the best detection performance on diffusion-model-generated images. Finally, the optimal performance on both detection and reasoning tasks is achieved when all three losses are applied.

\mathcal{L}_{LM}	\mathcal{L}_{FAC}	\mathcal{L}_{BCE}	DM	GAN	AVG \uparrow	CSS \uparrow
✓	×	×	92.33	79.67	86.00	0.61
✓	✓	×	93.75	80.83	87.29	0.75
✓	×	✓	96.00	81.67	88.84	0.63
✓	✓	✓	94.78	87.18	90.98	0.77

Table 5. Ablation study of multiple losses.

5.4. More Analysis

Visualization of FakeReasoning. We provide visualized results of forgery detection and reasoning results in Figure 4. Our method can accurately detect image authenticity as well as provide reliable reasoning on forgery-related attributes. Please refer to Appendix for more results.

Human Evaluation on Forgery Reasoning. To analyze the rationality of forgery reasoning, we randomly sample 100 images from each test set, score each sentence of forgery reasoning and average them. We use the 5-grade marking method, and the average score of forgery reasoning rationality is 4.19. Further analysis reveals a significant negative correlation between the rationality of forgery reasoning and the generative quality of the synthetic images.

Consistency Analysis of Forgery Detection. The inconsistency of LLMs [12, 46] poses a challenge for forgery detection task. To analyze the consistency of our method, we conduct 10 rounds of detection on MMFR evaluation sets with the initial temperature set at 0.2. The first inference (Round 0) serves as the baseline to track fluctuations in subsequent rounds. Our experiments show that the average accuracy fluctuation is 0.75%. We report detailed human evaluation and influence of temperature in the Appendix.

6. Conclusion

In this paper, we introduce the FDR-Task, a novel framework unifying authenticity detection and forgery reasoning for AI-generated images. To support this, we propose the MMFR-Dataset, a large-scale benchmark with hierarchical forgery reasoning annotations. Using this dataset, we develop FakeReasoning, a framework enhancing general-

ization and interpretability via Forgery-Aligned Contrastive Learning and a Classification Probability Mapper. Experiments across various generative models show that FakeReasoning consistently outperforms SOTA methods in both detection and reasoning tasks. Future work will extend this approach to multi-modal forgery detection and enhance its robustness under real-world distribution shifts, advancing reliable AI-generated content verification systems.

References

- [1] Josh Achiam, Steven Adler, Sandhini Agarwal, Lama Ahmad, Ilge Akkaya, Florencia Leoni Aleman, Diogo Almeida, Janko Altenschmidt, Sam Altman, Shyamal Anadkat, et al. Gpt-4 technical report. *arXiv preprint arXiv:2303.08774*, 2023. 7
- [2] Shuai Bai, Keqin Chen, Xuejing Liu, Jialin Wang, Wenbin Ge, Sibao Song, Kai Dang, Peng Wang, Shijie Wang, Jun Tang, Humen Zhong, Yuanzhi Zhu, Mingkun Yang, Zhaohai Li, Jianqiang Wan, Pengfei Wang, Wei Ding, Zheren Fu, Yiheng Xu, Jiabo Ye, Xi Zhang, Tianbao Xie, Zesen Cheng, Hang Zhang, Zhibo Yang, Haiyang Xu, and Junyang Lin. Qwen2.5-vl technical report. *arXiv preprint arXiv:2502.13923*, 2025. 4, 7
- [3] George Cazenavette, Avneesh Sud, Thomas Leung, and Ben Usman. Fakeinversion: Learning to detect images from unseen text-to-image models by inverting stable diffusion. In *Proceedings of the IEEE/CVF Conference on Computer Vision and Pattern Recognition*, pages 10759–10769, 2024. 1, 7
- [4] You-Ming Chang, Chen Yeh, Wei-Chen Chiu, and Ning Yu. Antifakeprompt: Prompt-tuned vision-language models are fake image detectors. *arXiv preprint arXiv:2310.17419*, 2023. 1, 2, 4, 6, 7
- [5] Baoying Chen, Jishen Zeng, Jianquan Yang, and Rui Yang. Drct: Diffusion reconstruction contrastive training towards universal detection of diffusion generated images. In *Forty-first International Conference on Machine Learning*, 2024. 1
- [6] Qiguang Chen, Libo Qin, Jin Zhang, Zhi Chen, Xiao Xu, and Wanxiang Che. M³ cot: A novel benchmark for multi-domain multi-step multi-modal chain-of-thought. *arXiv preprint arXiv:2405.16473*, 2024. 4
- [7] Zhe Chen, Jiannan Wu, Wenhai Wang, Weijie Su, Guo Chen, Sen Xing, Muyan Zhong, Qinglong Zhang, Xizhou Zhu, Lewei Lu, et al. Internvl: Scaling up vision foundation models and aligning for generic visual-linguistic tasks. In *Proceedings of the IEEE/CVF Conference on Computer Vision and Pattern Recognition*, pages 24185–24198, 2024. 4, 7
- [8] Davide Cozzolino, Giovanni Poggi, Riccardo Corvi, Matthias Nießner, and Luisa Verdoliva. Raising the Bar of AI-generated Image Detection with CLIP. In *Proceedings of the IEEE/CVF Conference on Computer Vision and Pattern Recognition Workshops*, pages 4356–4366, 2024. 4
- [9] Wenliang Dai, Junnan Li, Dongxu Li, Anthony Meng Huat Tiong, Junqi Zhao, Weisheng Wang, Boyang Li, Pascale Fung, and Steven Hoi. Instructblip: Towards general-purpose vision-language models with instruction tuning. *arXiv preprint arXiv:2305.06500*, 2023. 2, 7
- [10] Prafulla Dhariwal and Alexander Nichol. Diffusion models beat gans on image synthesis. *Advances in neural information processing systems*, 34:8780–8794, 2021. 1
- [11] Chengbo Dong, Xinru Chen, Ruohan Hu, Juan Cao, and Xirong Li. Mvss-net: Multi-view multi-scale supervised networks for image manipulation detection. *IEEE Transactions on Pattern Analysis and Machine Intelligence*, 45(3):3539–3553, 2022. 1
- [12] Yanai Elazar, Nora Kassner, Shauli Ravfogel, Abhilasha Ravichander, Eduard Hovy, Hinrich Schütze, and Yoav Goldberg. Measuring and improving consistency in pre-trained language models. *Transactions of the Association for Computational Linguistics*, 9:1012–1031, 2021. 8
- [13] Yueying Gao, Weiguo Lin, Junfeng Xu, Wanshan Xu, and Peibin Chen. Self-supervised adversarial training for robust face forgery detection. In *BMVC*, page 718, 2023. 6
- [14] Fabrizio Guillaro, Davide Cozzolino, Avneesh Sud, Nicholas Dufour, and Luisa Verdoliva. Trufor: Leveraging all-round clues for trustworthy image forgery detection and localization. In *Proceedings of the IEEE/CVF conference on computer vision and pattern recognition*, pages 20606–20615, 2023. 1
- [15] Xiao Guo, Xiaohong Liu, Zhiyuan Ren, Steven Grosz, Iacopo Masi, and Xiaoming Liu. Hierarchical fine-grained image forgery detection and localization. In *Proceedings of the IEEE/CVF Conference on Computer Vision and Pattern Recognition*, pages 3155–3165, 2023. 1
- [16] Kaiming He, Haoqi Fan, Yuxin Wu, Saining Xie, and Ross Girshick. Momentum contrast for unsupervised visual representation learning. In *Proceedings of the IEEE/CVF conference on computer vision and pattern recognition*, pages 9729–9738, 2020. 5
- [17] Evgeniy Hristoforu. Dalle-3. <https://huggingface.co/datasets/ehristoforu/dalle-3-images>, 2024. 4
- [18] Edward J Hu, Yelong Shen, Phillip Wallis, Zeyuan Allen-Zhu, Yuanzhi Li, Shean Wang, Lu Wang, and Weizhu Chen. Lora: Low-rank adaptation of large language models. *arXiv preprint arXiv:2106.09685*, 2021. 2, 7
- [19] Yonghyun Jeong, Doyeon Kim, Youngmin Ro, and Jongwon Choi. Frepgan: robust deepfake detection using frequency-level perturbations. In *Proceedings of the AAAI conference on artificial intelligence*, pages 1060–1068, 2022. 1
- [20] Shan Jia, Reilin Lyu, Kangran Zhao, Yize Chen, Zhiyuan Yan, Yan Ju, Chuanbo Hu, Xin Li, Baoyuan Wu, and Siwei Lyu. Can chatgpt detect deepfakes? a study of using multimodal large language models for media forensics. In *Proceedings of the IEEE/CVF Conference on Computer Vision and Pattern Recognition*, pages 4324–4333, 2024. 5
- [21] Tero Karras. Progressive growing of gans for improved quality, stability, and variation. *arXiv preprint arXiv:1710.10196*, 2017. 2
- [22] Mamadou Keita, Wassim Hamidouche, Hessen Bouguessa Eutamene, Abdelmalik Taleb-Ahmed, David Camacho, and Abdenour Hadid. Bi-lora: A vision-language approach

- for synthetic image detection. *Expert Systems*, 42(2):e13829, 2025. 2, 6
- [23] Prannay Khosla, Piotr Teterwak, Chen Wang, Aaron Sarna, Yonglong Tian, Phillip Isola, Aaron Maschiot, Ce Liu, and Dilip Krishnan. Supervised contrastive learning. *Advances in neural information processing systems*, 33:18661–18673, 2020. 5
- [24] Junnan Li, Dongxu Li, Silvio Savarese, and Steven Hoi. Blip-2: Bootstrapping language-image pre-training with frozen image encoders and large language models. In *International conference on machine learning*, pages 19730–19742. PMLR, 2023. 2, 3
- [25] Jiawei Li, Fanrui Zhang, Jiaying Zhu, Esther Sun, Qiang Zhang, and Zheng-Jun Zha. Forgerypt: Multimodal large language model for explainable image forgery detection and localization. *arXiv preprint arXiv:2410.10238*, 2024. 1
- [26] Lingzhi Li, Jianmin Bao, Hao Yang, Dong Chen, and Fang Wen. Faceshifter: Towards high fidelity and occlusion aware face swapping. *arXiv preprint arXiv:1912.13457*, 2019. 1
- [27] Xiaoming Li, Xinyu Hou, and Chen Change Loy. When stylegan meets stable diffusion: a w+ adapter for personalized image generation. In *Proceedings of the IEEE/CVF Conference on Computer Vision and Pattern Recognition (CVPR)*, pages 2187–2196, 2024. 1
- [28] Yixuan Li, Xuelin Liu, Xiaoyang Wang, Shiqi Wang, and Weisi Lin. Fakebench: Uncover the achilles’ heels of fake images with large multimodal models. *arXiv e-prints*, pages arXiv–2404, 2024. 3, 7
- [29] Haotian Liu, Chunyuan Li, Yuheng Li, and Yong Jae Lee. Improved baselines with visual instruction tuning. In *Proceedings of the IEEE/CVF Conference on Computer Vision and Pattern Recognition*, pages 26296–26306, 2024. 7
- [30] Haotian Liu, Chunyuan Li, Yuheng Li, Bo Li, Yuanhan Zhang, Sheng Shen, and Yong Jae Lee. Llava-next: Improved reasoning, ocr, and world knowledge, 2024. 4
- [31] Haotian Liu, Chunyuan Li, Qingyang Wu, and Yong Jae Lee. Visual instruction tuning. *Advances in neural information processing systems*, 36, 2024. 3, 6
- [32] Huan Liu, Zichang Tan, Chuangchuang Tan, Yunchao Wei, Jingdong Wang, and Yao Zhao. Forgery-aware adaptive transformer for generalizable synthetic image detection. In *Proceedings of the IEEE/CVF Conference on Computer Vision and Pattern Recognition*, pages 10770–10780, 2024. 1, 2
- [33] Zijun Long, George Killick, Richard McCreadie, and Gerardo Aragon Camarasa. Multiway-adapter: adapting multimodal large language models for scalable image-text retrieval. In *ICASSP 2024-2024 IEEE International Conference on Acoustics, Speech and Signal Processing (ICASSP)*, pages 6580–6584. IEEE, 2024. 5
- [34] Adam Novozamsky, Babak Mahdian, and Stanislav Saic. Imd2020: A large-scale annotated dataset tailored for detecting manipulated images. In *Proceedings of the IEEE/CVF winter conference on applications of computer vision workshops*, pages 71–80, 2020. 1
- [35] Utkarsh Ojha, Yuheng Li, and Yong Jae Lee. Towards universal fake image detectors that generalize across generative models. In *Proceedings of the IEEE/CVF Conference on Computer Vision and Pattern Recognition*, pages 24480–24489, 2023. 1, 2, 3, 4, 6, 7
- [36] Aaron van den Oord, Yazhe Li, and Oriol Vinyals. Representation learning with contrastive predictive coding. *arXiv preprint arXiv:1807.03748*, 2018. 5
- [37] Alec Radford, Jong Wook Kim, Chris Hallacy, Aditya Ramesh, Gabriel Goh, Sandhini Agarwal, Girish Sastry, Amanda Askell, Pamela Mishkin, Jack Clark, et al. Learning transferable visual models from natural language supervision. In *International conference on machine learning*, pages 8748–8763. PMLR, 2021. 2
- [38] Robin Rombach, Andreas Blattmann, Dominik Lorenz, Patrick Esser, and Björn Ommer. High-resolution image synthesis with latent diffusion models. In *Proceedings of the IEEE/CVF conference on computer vision and pattern recognition*, pages 10684–10695, 2022. 1
- [39] Olga Russakovsky, Jia Deng, Hao Su, Jonathan Krause, Sanjeev Satheesh, Sean Ma, Zhiheng Huang, Andrej Karpathy, Aditya Khosla, Michael Bernstein, Alexander C. Berg, and Li Fei-Fei. ImageNet Large Scale Visual Recognition Challenge. *International Journal of Computer Vision (IJCV)*, 115(3):211–252, 2015. 4
- [40] Axel Sauer, Katja Schwarz, and Andreas Geiger. Stylegan-xl: Scaling stylegan to large diverse datasets. In *ACM SIGGRAPH 2022 conference proceedings*, pages 1–10, 2022. 1
- [41] Christoph Schuhmann, Romain Beaumont, Richard Vencu, Cade Gordon, Ross Wightman, Mehdi Cherti, Theo Coombes, Aarush Katta, Clayton Mullis, Mitchell Wortsman, et al. Laion-5b: An open large-scale dataset for training next generation image-text models. *Advances in Neural Information Processing Systems*, 35:25278–25294, 2022. 3, 4
- [42] Ramprasaath R Selvaraju, Michael Cogswell, Abhishek Das, Ramakrishna Vedantam, Devi Parikh, and Dhruv Batra. Grad-cam: Visual explanations from deep networks via gradient-based localization. In *Proceedings of the IEEE international conference on computer vision*, pages 618–626, 2017. 1
- [43] Zeyang Sha, Zheng Li, Ning Yu, and Yang Zhang. De-fake: Detection and attribution of fake images generated by text-to-image generation models. In *Proceedings of the 2023 ACM SIGSAC Conference on Computer and Communications Security*, pages 3418–3432, 2023. 3, 6, 7
- [44] Hao Shao, Shengju Qian, Han Xiao, Guanglu Song, Zhuofan Zong, Letian Wang, Yu Liu, and Hongsheng Li. Visual cot: Advancing multi-modal language models with a comprehensive dataset and benchmark for chain-of-thought reasoning. *Advances in Neural Information Processing Systems*, 37:8612–8642, 2024. 4
- [45] Kaede Shiohara and Toshihiko Yamasaki. Detecting deep-fakes with self-blended images. In *Proceedings of the IEEE/CVF conference on computer vision and pattern recognition*, pages 18720–18729, 2022. 1
- [46] Rickard Stureborg, Dimitris Alikaniotis, and Yoshi Suhara. Large language models are inconsistent and biased evaluators. *arXiv preprint arXiv:2405.01724*, 2024. 8
- [47] Ilya Sutskever, Oriol Vinyals, and Quoc V Le. Sequence to sequence learning with neural networks. In *Advances in*

- Neural Information Processing Systems*. Curran Associates, Inc., 2014. 6
- [48] Chuangchuang Tan, Yao Zhao, Shikui Wei, Guanghua Gu, and Yunchao Wei. Learning on gradients: Generalized artifacts representation for gan-generated images detection. In *Proceedings of the IEEE/CVF Conference on Computer Vision and Pattern Recognition*, pages 12105–12114, 2023. 4
- [49] Gemini Team, Rohan Anil, Sebastian Borgeaud, Jean-Baptiste Alayrac, Jiahui Yu, Radu Soricut, Johan Schalkwyk, Andrew M Dai, Anja Hauth, Katie Millican, et al. Gemini: a family of highly capable multimodal models. *arXiv preprint arXiv:2312.11805*, 2023. 7
- [50] Justus Thies, Michael Zollhofer, Marc Stamminger, Christian Theobalt, and Matthias Nießner. Face2face: Real-time face capture and reenactment of rgb videos. In *Proceedings of the IEEE conference on computer vision and pattern recognition*, pages 2387–2395, 2016. 1
- [51] Justus Thies, Michael Zollhöfer, and Matthias Nießner. Deferred neural rendering: Image synthesis using neural textures. *Acm Transactions on Graphics (TOG)*, 38(4):1–12, 2019. 1
- [52] Haibo Wang and Weifeng Ge. Q&a prompts: Discovering rich visual clues through mining question-answer prompts for vqa requiring diverse world knowledge. In *European Conference on Computer Vision*, pages 274–292. Springer, 2024. 5
- [53] Sheng-Yu Wang, Oliver Wang, Richard Zhang, Andrew Owens, and Alexei A Efros. Cnn-generated images are surprisingly easy to spot... for now. In *Proceedings of the IEEE/CVF conference on computer vision and pattern recognition*, pages 8695–8704, 2020. 1, 2, 3, 4, 6, 7
- [54] Yabing Wang, Le Wang, Qiang Zhou, Zhibin Wang, Hao Li, Gang Hua, and Wei Tang. Multimodal llm enhanced cross-lingual cross-modal retrieval. In *Proceedings of the 32nd ACM International Conference on Multimedia*, pages 8296–8305, 2024. 5
- [55] Zhendong Wang, Jianmin Bao, Wengang Zhou, Weilun Wang, Hezhen Hu, Hong Chen, and Houqiang Li. Dire for diffusion-generated image detection. In *Proceedings of the IEEE/CVF International Conference on Computer Vision*, pages 22445–22455, 2023. 1, 2, 6, 7
- [56] Zijie J. Wang, Evan Montoya, David Munechika, Haoyang Yang, Benjamin Hoover, and Duen Horng Chau. DiffusionDB: A large-scale prompt gallery dataset for text-to-image generative models. *arXiv:2210.14896*, 2022. 3, 4
- [57] Bihan Wen, Ye Zhu, Ramanathan Subramanian, Tian-Tsong Ng, Xuanjing Shen, and Stefan Winkler. Coverage—a novel database for copy-move forgery detection. In *2016 IEEE international conference on image processing (ICIP)*, pages 161–165. IEEE, 2016. 1
- [58] Guowei Xu, Peng Jin, Li Hao, Yibing Song, Lichao Sun, and Li Yuan. Llava-o1: Let vision language models reason step-by-step. *arXiv preprint arXiv:2411.10440*, 2024. 4
- [59] Zhipei Xu, Xuanyu Zhang, Runyi Li, Zecheng Tang, Qing Huang, and Jian Zhang. Fakeshield: Explainable image forgery detection and localization via multi-modal large language models. *arXiv preprint arXiv:2410.02761*, 2024. 1, 3
- [60] Shilin Yan, Ouxiang Li, Jiayin Cai, Yanbin Hao, Xiaolong Jiang, Yao Hu, and Weidi Xie. A sanity check for ai-generated image detection. *arXiv preprint arXiv:2406.19435*, 2024. 1, 6, 7
- [61] Ning Yu, Larry S Davis, and Mario Fritz. Attributing fake images to gans: Learning and analyzing gan fingerprints. In *Proceedings of the IEEE/CVF international conference on computer vision*, pages 7556–7566, 2019. 1
- [62] Xingchen Zeng, Haichuan Lin, Yilin Ye, and Wei Zeng. Advancing multimodal large language models in chart question answering with visualization-referenced instruction tuning. *IEEE Transactions on Visualization and Computer Graphics*, 2024. 5
- [63] Xian Zhang, Haokun Wen, Jianlong Wu, Pengda Qin, Hui Xue', and Liqiang Nie. Differential-perceptive and retrieval-augmented mllm for change captioning. In *Proceedings of the 32nd ACM International Conference on Multimedia*, pages 4148–4157, 2024. 5
- [64] Yue Zhang, Ben Colman, Xiao Guo, Ali Shahriyari, and Gaurav Bharaj. Common sense reasoning for deepfake detection. In *European Conference on Computer Vision*, pages 399–415. Springer, 2024. 1
- [65] Zicheng Zhang, Haoning Wu, Chunyi Li, Yingjie Zhou, Wei Sun, Xiongkuo Min, Zijian Chen, Xiaohong Liu, Weisi Lin, and Guangtao Zhai. A-bench: Are llms masters at evaluating ai-generated images? *arXiv preprint arXiv:2406.03070*, 2024. 3
- [66] Henry Hengyuan Zhao, Pan Zhou, Difei Gao, Zechen Bai, and Mike Zheng Shou. Lova3: Learning to visual question answering, asking and assessment. *Advances in Neural Information Processing Systems*, 37:115146–115175, 2025. 5
- [67] Nan Zhong, Yiran Xu, Zhenxing Qian, and Xinpeng Zhang. Rich and poor texture contrast: A simple yet effective approach for ai-generated image detection. *CoRR*, 2023. 3
- [68] Mingjian Zhu, Hanting Chen, Qiangyu Yan, Xudong Huang, Guanyu Lin, Wei Li, Zhijun Tu, Hailin Hu, Jie Hu, and Yunhe Wang. Genimage: A million-scale benchmark for detecting ai-generated image. *Advances in Neural Information Processing Systems*, 36:77771–77782, 2023. 3

A. Appendix

A.1. More Ablation Studies

In the proposed FakeReasoning, we fine-tune the projection layer and the large language model. In this section, we conduct further ablation study on the fine-tuning modules and trainable parameters. Results are shown in Table 6. Simultaneously updating the parameters of the projection layer and the large language model can achieve optimal performance on both detection and reasoning tasks.

A.2. More Analysis on LLM

LLM plays an important role in the proposed FakeReasoning. In this section, we provide a detailed analysis of the reasoning rationality and detection consistency.

Human Evaluation on Forgery Reasoning. As outlined in Section 5.4, we randomly sampled 100 images from each evaluation set to perform forgery detection and reasoning using FakeReasoning. From the reasoning stage, each sentence is evaluated using a five-point marking method to assess its rationality, where a score of 5 indicates highly rational reasoning and 1 indicates highly irrational reasoning. We then compute the average score for each evaluation set. In accordance with the order of evaluation sets in Table 1, the rationality scores are 4.14, 4.00, 4.20, 3.83, 4.07, 4.29, 4.92, 3.18, 4.83, and 4.09. The results demonstrate a negative correlation between the rationality of forgery reasoning and the quality of synthetic images. When the generative quality is low, FakeReasoning provides specific reasoning based on image content. However, as the generative quality improves, FakeReasoning tends to produce more stereotypical reasoning outcomes.

Consistency Analysis of Forgery Detection. As mentioned in Section 5.4, we first conduct 10 rounds of inference on evaluation sets with the original temperature 0.2. The first inference (Round 0) serves as the baseline to track fluctuations in subsequent rounds. The results, presented in Table 7, showing an average fluctuation of 0.75%.

Temperature regulates the randomness in text generation. Higher values lead to more random and diverse outputs, while lower values yield more deterministic and conservative results. Therefore, we conduct experiments on the impact of the temperature in forgery detection. The temperature is set to 0.1, 0.2, 0.3, 0.4, 0.5 and 0.6. Results are shown in Table 8. When the temperature is set to 0.1 and 0.2, the average fluctuation remains below 1%. Optimal detection accuracy is achieved at a temperature of 0.2. As the temperature increases, fluctuations become more pronounced. With similar performance of fluctuation and accuracy, we examine forgery attribute reasoning at temperatures of 0.1 and 0.2. At a temperature of 0.1, forgery reasoning exhibits higher content similarity and greater stereotypical patterns compared to 0.2.

Projection	LLM	Parameters	DM	GAN	AVG \uparrow	CSS \uparrow
✓	×	31M	93.58	83.33	90.17	0.64
×	✓	501M	93.25	79.33	88.61	0.71
✓	✓	532M	94.78	87.18	90.98	0.77

Table 6. Ablation study of fine-tuning modules.

Round	Fluctuation	Round	Fluctuation	Round	Fluctuation
1	1.30%	2	0.55%	3	1.10%
4	0.55%	5	0.55%	6	1.10%
7	0.55%	8	0.55%	9	0.55%

Table 7. Consistency analysis. Ten round inferences are conducted with the original temperature 0.2.

Temp.	Fluct.	ACC	Temp.	Fluct.	ACC
0.1	0.54%	89.60	0.2	0.75%	90.98
0.3	3.19%	89.50	0.4	1.39%	88.70
0.5	2.19%	89.20	0.6	3.10%	88.40

Table 8. Consistency analysis on temperatures. Ten round inferences are conducted with each temperature.

A.3. Dataset Details

A.3.1. Dataset Statistics

The training set consists of 50,268 synthetic images with 129,351 reasoning annotations, and 50,909 real images with 183,245 reasoning annotations. Figure 5 shows the distribution of text length from the caption and reasoning stages. Through tailored prompt engineering, we obtain detailed annotations on forgery attributes for the FDR-Task. Across all annotations, there are 10 types of forgery-related attributes, whose distributions in real and fake images are depicted in Figure 5.

A.3.2. Forgery Interpretation Prompts

For real and fake images, we design distinct prompts, instructing GPT-4o to interpret specific attributes signifying the image authenticity. The full-text prompts are illustrated in Figure 6 and Figure 7.

A.3.3. Examples

We present more examples (images with forgery reasoning CoT) from the Multi-Modal Forgery Reasoning Dataset in Figure 8. With detailed and structured forgery reasoning, VLMs can gain deeper insights into forgery-related semantics and low-level forgeries within AI-generated images.

A.4. More Visualization Results

We provide more visualization results on evaluation sets. All of detection and reasoning results in Figures 9 and 10 can be achieved by the proposed FakeReasoning.

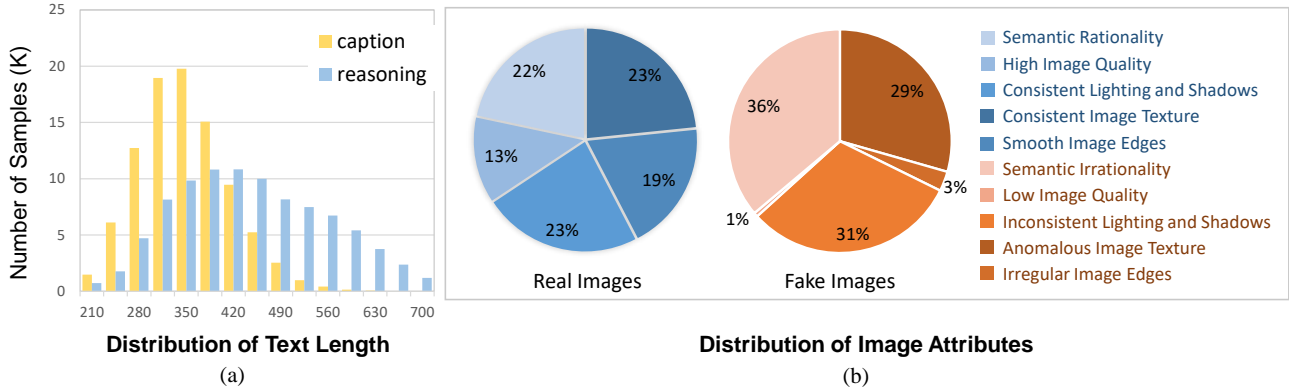


Figure 5. Statistics of MMFR-Dataset. (a) Distribution of text length; (b) Image attributes distribution of real and fake images.

Task: Here is a **fake** image and it is **AI-generated**. You are an image forensic expert tasked with describing forgery attributes of fake images. The image is known to be AI-generated, which can include photos, artworks, digital images, etc. Therefore, do not judge the authenticity based on the type of image. Your focus should be on identifying specific forgery attributes.

Instructions:

1. Forgery Attributes: A knowledge base has been provided with common forgery attributes: {"**Inconsistent Lighting and Shadows**", "**Irregular Image Edges**", "**Anomalous Image Texture**", "**Low Image Quality**", "**Semantic Irrationality**"}. There are five main types, but not every fake image will exhibit all of them. Find existing forgery attributes of the image, and describe these forgery attributes.
2. Output Format:
 - If you find forgery attributes, describe them and output: {
 "Answer": "The image is fake.",
 "Forgery Attributes": {
 "<type of forgery attribute>": "<describe forgery attribute>",
 }
 }
 - If you are unable to determine if the image is real or fake, output: {"Answer": "Can not determine if the image is real or fake."}

Figure 6. Full-text prompt for GPT-4o to interpret fake images.

Task: Here is a **real** image, which is captured or created from the real world, as opposed to being artificially generated by an AI system. You are an image forensic expert tasked with: describing the image content, analyzing the image attributes and deciding why this image is real instead of manipulated or AI-generated.

Instructions: A knowledge base has been provided with common image attributes: {"**Consistent Lighting and Shadows**", "**Smooth and Natural Image Edges**", "**Natural and Consistent Image Texture**", "**High Image Quality**", "**Semantic Rationality**"}. There are five main types. Find according attributes proving the image authenticity and describe these attributes.

Output Format: Only output in the following JSON format.

- If you find image attributes proving the image authenticity, describe them and output: {
 "Answer": "The image is real.",
 "Attributes": {
 "<type of image attribute>": "<describe image attribute>",
 }
 }
- If you are unable to determine if the image is real or fake, output: {"Answer": "Can not determine if the image is real or fake."}

Figure 7. Full-text prompt for GPT-4o to interpret real images.



Is this image real or fake? Please describe the image, reasoning step-by-step and conclude with 'this image is real' or 'this image is fake'.

<SUMMARY> I will determine if the image is real or fake by analyzing its content and identifying forgery attributes from both low-level and high-level perspectives. I will then conclude by stating either 'this image is real' or 'this image is fake' based on my analysis. </SUMMARY>

<CAPTION> The image depicts a highly detailed, surreal portrait of a person with long, dark hair and striking, golden eyes. The face is adorned with intricate, organic patterns that resemble veins or roots, adding a mystical and otherworldly quality to the artwork. The background features a monochromatic, textured design that complements the surreal theme of the portrait. </CAPTION>

<REASONING> From low-level perspective: The lighting on the face does not match the lighting on the background and other elements, indicating inconsistency. The skin texture appears more like a computer-generated texture rather than realistic human skin. From high-level perspective: The image depicts a person with unnatural plant-like elements growing from their face, which is not possible in reality. Therefore, this image is fake. </REASONING>

<CONCLUSION> Based on the analysis above, this image is fake.</CONCLUSION>



Is this image real or fake? Please describe the image, reasoning step-by-step and conclude with 'this image is real' or 'this image is fake'.

<SUMMARY> I will determine if the image is real or fake by analyzing its content and identifying forgery attributes from both low-level and high-level perspectives. I will then conclude by stating either 'this image is real' or 'this image is fake' based on my analysis. </SUMMARY>

<CAPTION> The image depicts a serene, dreamlike scene with vibrant autumn foliage in shades of red, orange, and purple. A person is rowing a boat on a calm, reflective body of water, surrounded by misty trees. The setting sun casts a warm, golden glow, creating a peaceful and magical atmosphere. In the background, there's a large, classical-style building partially obscured by the trees. </CAPTION>

<REASONING> From low-level perspective: The lighting on the trees and water does not align with the visible light sources, leading to unrealistic shadow directions and intensities. The texture of the foliage and the water surface appears overly smooth and lacks natural detail, which can be indicative of AI-generated images. From high-level perspective: The scene depicts an unrealistic setting with overly vibrant and hyper-saturated colors in the trees and sky, creating an unnatural appearance. Therefore, this image is fake. </REASONING>

<CONCLUSION> Based on the analysis above, this image is fake.</CONCLUSION>



Is this image real or fake? Please describe the image, reasoning step-by-step and conclude with 'this image is real' or 'this image is fake'.

<SUMMARY> I will determine if the image is real or fake by analyzing its content and identifying forgery attributes from both low-level and high-level perspectives. I will then conclude by stating either 'this image is real' or 'this image is fake' based on my analysis. </SUMMARY>

<CAPTION> The image shows two people posing in front of a wall decorated with triangular flags. The person on the left is wearing a black dress and high heels, while the person on the right is dressed in a dark suit with a hat. They appear to be in a playful or celebratory mood, possibly at a themed event or party. </CAPTION>

<REASONING> From low-level perspective: The texture of clothing and wall surfaces appears consistent and realistic. The edges of the subjects and objects are smooth and coherent, with no unnatural transitions. The lighting falls naturally across the scene, with appropriate shadows. From high-level perspective: The individuals are posed naturally, suggesting a real moment captured. Therefore, this image is real. </REASONING>

<CONCLUSION> Based on the analysis above, this image is real.</CONCLUSION>



Is this image real or fake? Please describe the image, reasoning step-by-step and conclude with 'this image is real' or 'this image is fake'.

<SUMMARY> I will determine if the image is real or fake by analyzing its content and identifying forgery attributes from both low-level and high-level perspectives. I will then conclude by stating either 'this image is real' or 'this image is fake' based on my analysis.</SUMMARY>

<CAPTION> The image shows a wooden gazebo with a slanted roof and a stone countertop, likely serving as an outdoor bar or kitchen area. It is surrounded by a well-maintained lawn and features decorative elements like hanging plants and a black lamppost. The setting appears to be a backyard with a wooden fence in the background. </CAPTION>

<REASONING> From low-level perspective: The textures of wood, stone, and foliage appear natural and realistic. The edges of the objects, such as the gazebo and furniture, are clear and smoothly integrated into the scene. The lighting is uniform with natural shadows cast by the structures, indicating a realistic outdoor setting. The image has good resolution with clear details, enhancing its authenticity. From high-level perspective: The scene shows a well-organized backyard with elements that are logically placed and commonly found in such settings. Therefore, this image is real. </REASONING>

<CONCLUSION> Based on the analysis above, this image is real.</CONCLUSION>

Figure 8. More examples of images with forgery reasoning CoT from the proposed MMFR-Dataset.



Figure 9. More visualization results of the proposed FakeReasoning.

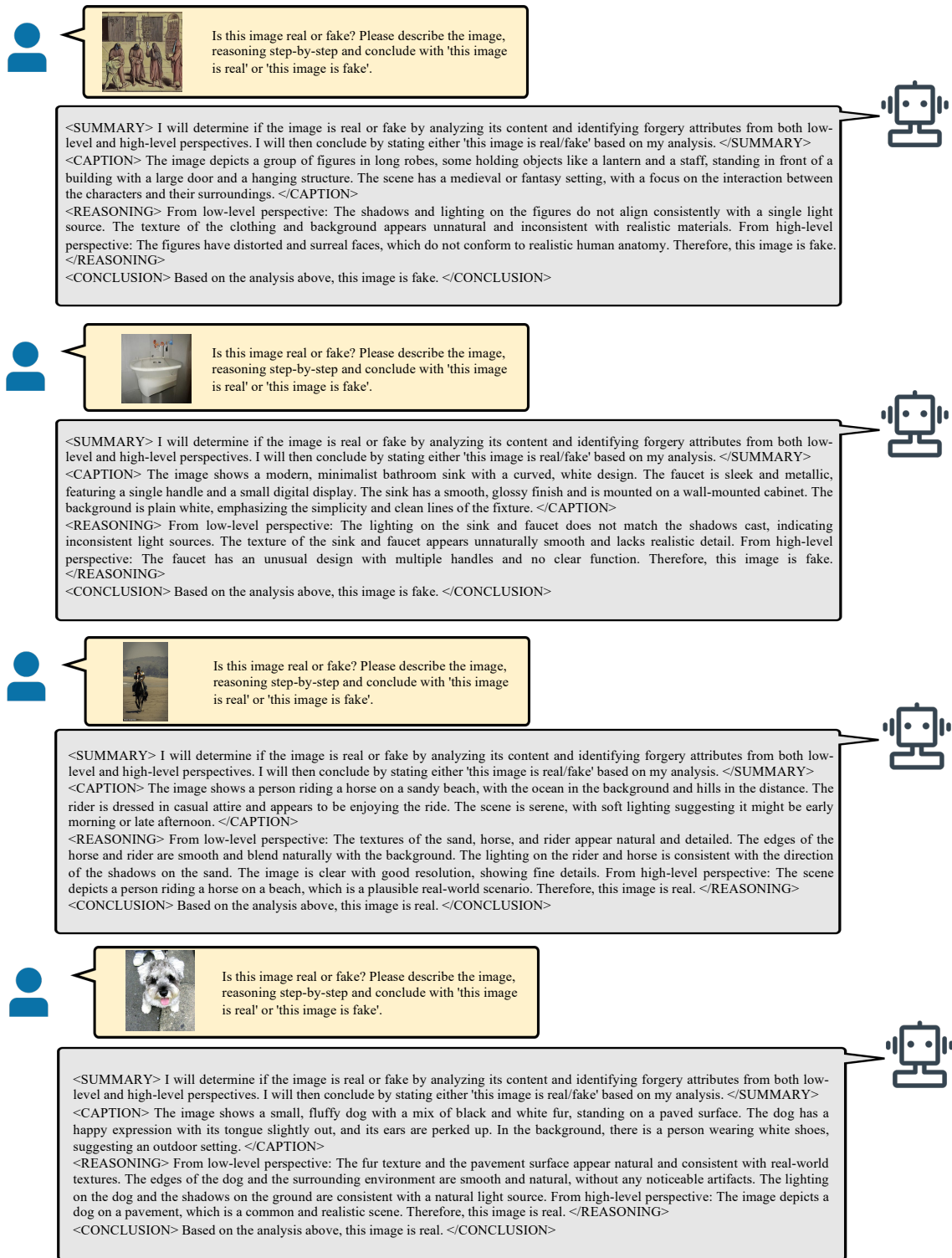


Figure 10. More visualization results of the proposed FakeReasoning.